Fluctuations and criticality in the random-field Ising model

Panagiotis E. Theodorakis
Department of Chemical Engineering, Imperial College London, London SW7 2AZ, United Kingdom

Ioannis Georgiou
Institute for Theoretical Physics and Center for Computational Materials Science, Vienna University of Technology, Wiedner Hauptstraße 8-10, A-1040 Vienna, Austria

Nikolaos G. Fytas*
Department of Physics, University of Athens, Panepistimiopolis, GR 15784 Zografos, Athens, Greece and Applied Mathematics Research Centre, Coventry University, Coventry, CV1 5FB, United Kingdom

(Received 17 December 2012; revised manuscript received 4 February 2013; published 8 March 2013)

We investigate the critical properties of the $d = 3$ random-field Ising model with a Gaussian field distribution at zero temperature. By implementing suitable graph-theoretical algorithms, we perform a large-scale numerical simulation of the model for a vast range of values of the disorder strength h and system sizes $\mathcal{V} = L \times L \times L$, with $L \leqslant 156$. Using the sample-to-sample fluctuations of various quantities and proper finite-size scaling techniques we estimate with high accuracy the critical disorder strength h_c and the correlation length exponent ν. Additional simulations in the area of the estimated critical-field strength and relevant scaling analysis of the bond energy suggest bounds for the specific heat critical exponent α and the violation of the hyperscaling exponent θ. Finally, a data collapse analysis of the order parameter and disconnected susceptibility provides accurate estimates for the critical exponent ratios β/ν and $\bar{\gamma}/\nu$, respectively.

DOI: 10.1103/PhysRevE.87.032119 PACS number(s): 05.50.+q, 75.10.Hk, 64.60.Cn, 75.10.Nr

I. INTRODUCTION

The random-field Ising model (RFIM) is one of the archetypal disordered systems [1–11], extensively studied due to its theoretical interest, as well as its close connection to experiments in hard [12–15] and soft condensed matter systems [16]. Its beauty is that the mixture of random fields and the standard Ising model creates rich physics and leaves many still unanswered problems. The Hamiltonian describing the model is

$$\mathcal{H} = -J \sum_{\langle i,j \rangle} \sigma_i \sigma_j - \sum_i h_i \sigma_i, \tag{1}$$

where $\sigma_i = \pm 1$ are Ising spins, $J > 0$ is the nearest neighbor's ferromagnetic interaction, and h_i are independent quenched random fields. Several field distributions have been considered in the literature, the most common ones being the Gaussian and bimodal distributions [14,17–19].

The existence of an ordered ferromagnetic phase for the RFIM, at low temperature and weak disorder, followed from the seminal discussion of Imry and Ma [1], when the space dimension is greater than two ($d > 2$) [17–21]. This has provided us with a general qualitative agreement on the sketch of the phase boundary, separating the ordered ferromagnetic phase from the high-temperature paramagnetic one. The phase-diagram line separates the two phases of the model and intersects the randomness axis at the critical value of the disorder strength h_c, as shown in Fig. 1. Such qualitative sketching has been commonly used in most papers for the RFIM [22–27], and closed form quantitative expressions are also known from the early mean-field calculations [27]. However, it is generally true that the quantitative aspects of phase diagrams produced by mean-field treatments are very poor approximations.

The criteria for determining the order of the low-temperature phase transition and its dependence on the form of the field distribution have been discussed through the years [27–34]. In fact, different results have been proposed for different field distributions, like the existence of a tricritical point at the strong disorder regime of the system, present only in the bimodal case [27,30]. Currently, despite the huge efforts recorded in the literature, a clear picture of the model's critical behavior is still lacking. Although the view that the phase transition of the RFIM is of second order is well established [35–38], the extremely small value of the exponent β continues to cast some doubts. Moreover, a rather strong debate exists with regard to the role of disorder: The available simulations are not able to settle the question of whether the critical exponents depend on the particular choice of the distribution for the random fields, analogously to the mean-field theory predictions [27]. Thus, the whole issue of the model's critical behavior is under intense investigation [35–49].

The scope of the present work is to shed some light in this direction by examining several critical features of the phase diagram of the RFIM at $d = 3$. To this end, we recruit powerful numerical and finite-size scaling (FSS) techniques in order to obtain accurate numerical data through the extensive use of large simulation platforms. On technical grounds, we implement well-established optimization methods at zero temperature ($T = 0$) combined with a Gaussian distribution of random fields, as given by the formula

$$\mathcal{P}(h_i) = \frac{1}{\sqrt{2\pi h^2}} \exp\left(-\frac{h_i^2}{2h^2}\right). \tag{2}$$

*nfytas@phys.uoa.gr

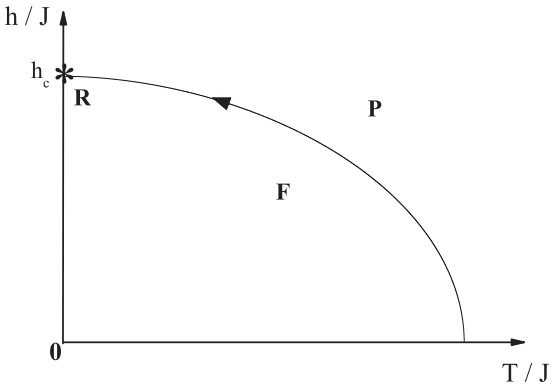

FIG. 1. Schematic phase diagram and renormalization-group flow of the RFIM. The solid line separates the ferromagnetic (**F**) and paramagnetic (**P**) phases. The black arrow shows the flow to the random fixed point (**R**) at $T = 0$ and $h = h_c$, as marked by an asterisk.

The main advantage of the above distribution (2) is that the ground state of the system is nondegenerate, so it is sufficient to calculate just one ground state in order to get the necessary information. Note here that, for cases of discrete distributions, like the bimodal, degeneracy complicates the numerical solution of the system at $T = 0$, since one has to sweep over all the possible ground states of the system [50,51]. On physical grounds, our attempt benefits from classical FSS techniques and a scaling approach that involves the sample-to-sample fluctuations of several quantities of the system. In particular, sample-to-sample fluctuations and the relative issue of self-averaging have attracted much interest in the study of disordered systems [52]. Although it has been known for many years now that for (spin and regular) glasses there is no self-averaging in the ordered phase [53], for random ferromagnets such behavior was first observed for the RFIM by Dayan *et al.* [54] and some years later for the random versions of the Ising and Ashkin-Teller models [55,56]. Ever since, the subject of breakdown of self-averaging has been an important aspect of several theoretical and numerical investigations of disordered spin systems [57–69]. In view of this increasing interest, we discuss here another successful alternative approach to the criticality of the RFIM via its sample-to-sample fluctuations at $T = 0$.

The rest of the paper is organized as follows: In the next section we describe briefly the numerical approach, and we provide all the necessary details of our investigation. The relevant FSS analysis of the numerical data is discussed in Sec. III. In particular, in this section we give refined estimates of the critical disorder strength h_c and the critical exponent ν via a new approach based on the sample-to-sample fluctuations of the model. We also present results on the controversial issue of the specific heat of the RFIM by studying the scaling behavior of the bond energy at the estimated critical field value and its close neighborhood. Finally, a data collapse analysis of the order parameter and magnetic susceptibility corroborates our obtained values for h_c and ν and provides us with estimates for the magnetic exponent ratios β/ν and $\bar{\gamma}/\nu$, respectively. Finally, the paper ends with a summary of our conclusions in Sec. IV.

II. SIMULATION PROTOCOL

As already discussed extensively in the literature (see Refs. [70,71], and references therein), the RFIM captures essential features of models in statistical physics that are controlled by disorder and have frustration. Such systems show complex energy landscapes due to the presence of large barriers that separate several metastable states. If such models are studied using simulations mimicking the local dynamics of physical processes, it takes an extremely long time to encounter the exact ground state. However, there are cases where efficient methods for finding the ground state can be utilized, and, fortunately, the RFIM is one such clear case. These methods escape from the typical direct physical representation of the system, in a way that extra degrees of freedom are introduced and an expanded problem is finally solved. By expanding the configuration space and choosing proper dynamics, the algorithm practically avoids the need of overcoming large barriers that exist in the original physical configuration space. An attractor state in the extended space is found in time polynomial in the size of the system, and when the algorithm terminates, the relevant auxiliary fields can be projected onto a physical configuration, which is the guaranteed ground state.

The random field is a relevant perturbation at the pure fixed point, and the random-field fixed point is at $T = 0$ [14,17–20]. Hence, the critical behavior is the same everywhere along the phase boundary of Fig. 1, and we can predict it simply by staying at $T = 0$ and crossing the phase boundary at $h = h_c$. This is a convenient approach because we can determine the ground states of the system exactly using efficient optimization algorithms [50,51,72–85] through an existing mapping of the ground state to the maximum-flow optimization problem [86–88]. A clear advantage of this approach is the ability to simulate large system sizes and disorder ensembles in rather moderate computational times. We should underline here that even the most efficient $T > 0$ Monte Carlo schemes exhibit extremely slow dynamics in the low-temperature phase of these systems and are upper bounded by linear sizes of the order of $L_{\max} \leqslant 32$ [70,71]. Further assets in the $T = 0$ approach are the absence of statistical errors and equilibration problems, which, on the other hand, are the two major drawbacks encountered in the $T > 0$ simulation of systems with rough free-energy landscapes [14].

The application of maximum-flow algorithms to the RFIM is nowadays well established [80]. The most efficient network flow algorithm used to solve the RFIM is the push-relabel algorithm of Tarjan and Goldberg [89]. For the interested reader, general proofs and theorems on the push-relabel algorithm can be found in standard textbooks [87,88]. The version of the algorithm implemented in our study involves a modification proposed by Middleton *et al.* [35,77,78] that removes the source and sink nodes, reducing memory usage and clarifying the physical connection [77,78].

The algorithm starts by assigning an excess x_i to each lattice site i, with $x_i = h_i$. Residual capacity variables r_{ij} between neighboring sites are initially set to J. A height variable u_i is then assigned to each node via a global update step. In this global update, the value of u_i at each site in the set $\mathcal{T} = \{j | x_j < 0\}$ of negative excess sites is set to zero. Sites with $x_i \geqslant 0$ have u_i set to the length of the shortest path,

via edges with positive capacity, from i to $\mathcal{T}$. The ground state is found by successively rearranging the excesses x_i, via push operations, and updating the heights, via relabel operations. When no more pushes or relabels are possible, a final global update determines the ground state, so that sites which are path connected by bonds with $r_{ij} > 0$ to $\mathcal{T}$ have $\sigma_i = -1$, while those which are disconnected from $\mathcal{T}$ have $\sigma_i = 1$. A push operation moves excess from a site i to a lower height neighbor j, if possible, that is, whenever $x_i > 0$, $r_{ij} > 0$, and $u_j = u_i - 1$. In a push, the working variables are modified according to $x_i \to x_i - \delta$, $x_j \to x_j + \delta$, $r_{ij} \to r_{ij} - \delta$, and $r_{ji} \to r_{ji} + \delta$, with $\delta = \min(x_i, r_{ij})$. Push operations tend to move the positive excess towards sites in $\mathcal{T}$. When $x_i > 0$ and no further push is possible, the site is relabeled, with u_i increased to $1 + \min_{\{j|r_{ij}>0\}} u_j$. In addition, if a set of highest sites $\mathcal{U}$ becomes isolated, with $u_i > u_j + 1$, for all $i \in \mathcal{U}$ and all $j \notin \mathcal{U}$, the height u_i for all $i \in \mathcal{U}$ is increased to its maximum value, $\mathcal{V}$, as these sites will always be isolated from the negative excess nodes. Last but not least, the computational efficiency of the algorithm has been increased via the use of periodic global updates every $\mathcal{V}$ relabels [77,78].

Using the above described version of the push-relabel algorithm we performed large-scale simulations of the Gaussian RFIM for a wide range of simulation parameters. In the first part, preliminary runs were executed, including also small systems sizes $\mathcal{V} \leqslant 20^3$, in order to probe efficiently the critical h regime of the model. In the second part, extensive simulations have been performed for lattice sizes $L \in \{24,32,48,64,78,96,128,156\}$ and disorder strengths $h \in [2.0 - 3.0]$ with a step $\delta h = 0.02$. For each pair $(L;h)$ an extensive disorder averaging $[\cdots]$ process has been undertaken, by sampling over 50×10^3 independent random-field realizations, much larger than in previous relevant studies of the model [35,74,79]. Finally, in most of the figures below, error bars are smaller than the system size and therefore are indistinguishable.

III. FINITE-SIZE SCALING ANALYSIS

As the outcome of the push-relabel algorithm is the spin configuration of the ground state, we can calculate for a given sample of a lattice with linear size L the magnetization via $m = \mathcal{V}^{-1} \sum_i \sigma_i$. Taking the average over different disorder configurations we may define the order parameter of the system $M = [|m|]$ and the disconnected susceptibility $\chi_{\rm dis} = \mathcal{V}[m^2]$. Another physical parameter of interest is the bond energy per spin that corresponds to the first term of the Hamiltonian (1), i.e., $e_{\rm J} = -\mathcal{V}^{-1} \sum_{\langle i,j \rangle} \sigma_i \sigma_j$, and its disorder average, defined hereafter as $E_{\rm J} = [e_{\rm J}]$. Our analysis in the sequel will be mainly based on these three thermodynamic quantities. In particular, the disorder-averaged bond energy will be used for an investigation of the critical behavior of the specific heat of the RFIM.

At this point, let us start the presentation of our FSS approach with Fig. 2, where we plot the sample-to-sample fluctuations over disorder of three quantities, of physical and technical origin. In particular, we plot the fluctuations of the order parameter M [panel (a)], the bond energy $E_{\rm J}$ [panel (b)], and the number of primitive operations of the push-relabel algorithm, that is, the number of relabels per spin R [panel (c)].

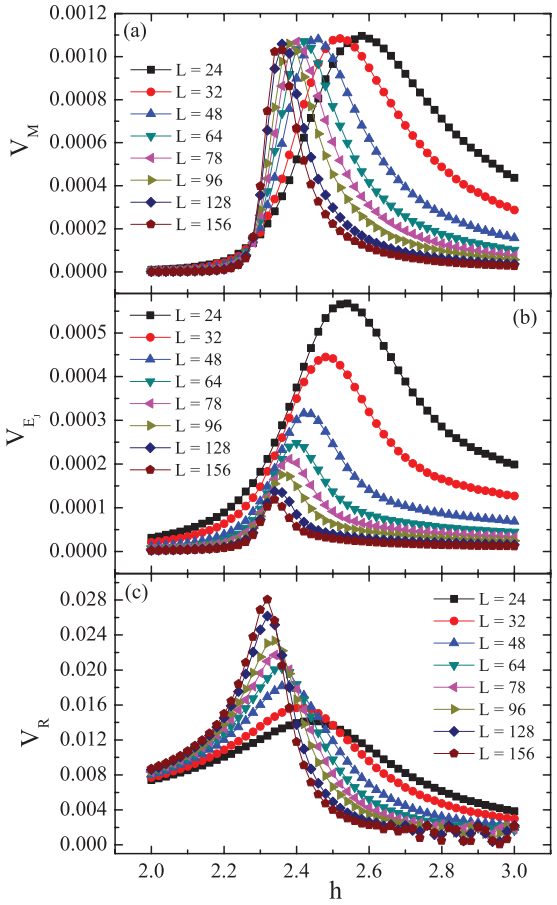

FIG. 2. (Color online) Sample-to-sample fluctuations of the order parameter V_M (a), bond energy $V_{E_{\rm J}}$ (b), and number of relabel operations per spin V_R (c), of the Gaussian RFIM as a function of the disorder strength for various lattice sizes in the range $L = 24$–156. Lines are simple guides to the eye.

All these fluctuations are plotted as a function of the disorder strength h for the complete lattice size range $L = 24$–156. It is clear that for every lattice size L, these fluctuations appear to have a maximum value at a certain value of h, denoted hereafter as $h^*_{\rm L}$, that may be considered in the following as a suitable pseudocritical disorder strength. By fitting the data points around the maximum first to a Gaussian, and subsequently to a fourth-order polynomial, we have extracted the values of the peak locations ($h^*_{\rm L}$) by taking the mean value via the two fitting functions, as well as the corresponding error bars. Using now these values for $h^*_{\rm L}$ we consider in the main panel of Fig. 3 a simultaneous power-law fitting attempt of the form

$$h^*_{\rm L} = h_{\rm c} + bL^{-1/\nu}, \tag{3}$$

simultaneous meaning that the values of $h_{\rm c}$ and ν for all data sets in the fitting procedure are shared in the fit. The quality of the fit is fair enough, with a value of χ^2/d.o.f. of the order of 0.75, where d.o.f. refers to the degrees of freedom and produces the estimates $h_{\rm c} = 2.2725(25)$ and $\nu = 1.379(24)$ for the critical disorder strength and the correlation length exponent. These values compare very well to the most accurate estimates of the literature $h_{\rm c} = 2.270(4)$ and $\nu = 1.37(9)$, as given by Middleton and Fisher [35].

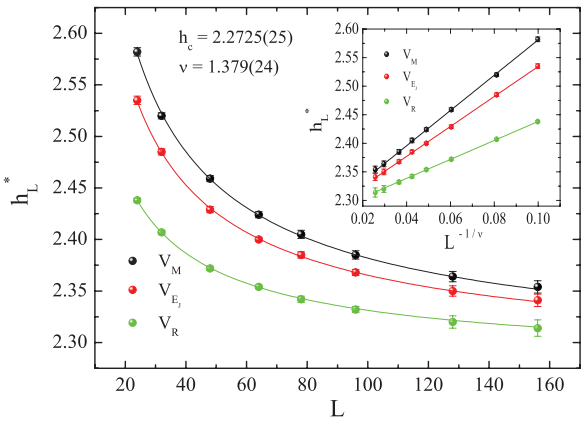

FIG. 3. (Color online) Simultaneous fitting of the form (3) of the pseudocritical disorder strengths h_{L}^{*}, obtained from the peak positions of the fluctuations shown in Fig. 2. The shared parameters of the three data sets of the fit are the critical strength h_{c} and the correlation length exponent ν. The inset shows the data as a function of $L^{-1/\nu}$.

Having simulated eight lattice size points, we also tried to perform the above analysis including higher-order scaling corrections of the form $(1 + b'L^{-\omega})$, where ω is the well-known correction-to-scaling exponent. As it is well known, the role of scaling corrections in the study of universality classes is of paramount importance. Although for the equilibrium properties of the RFIM the presence, and effects, of scaling corrections in the critical behavior of its thermodynamic properties have been disregarded, for the out-of-equilibrium version of the RFIM it has been shown that the election of the scaling variable is causing the major source of uncertainty in the determination of h_{c} and relevant exponents [90]. Thus, we attempted to perform a global fitting with the data of Fig. 3 using now the revised formula $h_{\mathrm{L}}^{*} = h_{\mathrm{c}} + bL^{-1/\nu}(1 + b'L^{-\omega})$, sharing as before the values of h_{c} and ν, and also the value of ω in this case, for the three data sets. However, no improvement has been observed in the quality of the fit. On the contrary, the corrected scaling assumption resulted in an unstable fitting procedure with significantly large errors in the values of the exponent ν and the coefficient b', as well as the exponent ω. Note that, such a behavior was also observed when fitting separately the numerical data for the fluctuations of M, E_{J}, and R (see also the discussion below).

We note here that our suggestion of choosing these newly defined pseudocritical disorder strengths h_{L}^{*} as a proper measure for performing FSS closely follows the analogous considerations of Hartmann and Young [74] and Dukovski and Machta [79], also for the Gaussian RFIM. The first authors [74] considered pseudocritical disorder strengths at the values of h at which a specific-heat-like quantity obtained by numerically differentiating the bond energy with respect to h attains its maximum. On the other hand, the authors of Ref. [79] identified the pseudocritical points as those in the H-h plane (with H a uniform external field), where three degenerate ground states of the system show the largest discontinuities in the magnetization. It appears that this method of extracting pseudocritical points from the maxima of some properly defined thermodynamic quantity is capable of producing very accurate estimates for both the critical disorder strength and the correlation length exponent, assuming that its behavior follows the observed shift behavior of our pseudocritical disorder strengths h_{L}^{*}. It is well known from the general scaling theory that, even for simple models, the equality between the correlation length exponent and the shift exponent is not a necessary consequence of scaling [91]. Of course, it is a general practice to assume that the correlation length behavior can be deduced by the shift of appropriate thermodynamic functions.

Middleton and Fisher [35], using similar reasoning on the Gaussian RFIM, characterized the distribution of the order parameter by the average over samples of the square of the magnetization per spin and the root-mean-square sample-to-sample variations of the square of the magnetization. They identified a similar behavior to that of Fig. 2, i.e., with increasing L, the peak magnitude of this quantity moved its location to smaller values of h, defining another relevant pseudocritical disorder strength. However, in Ref. [35] the authors were interested only in the scaling behavior of the height of these peaks. The practice followed in the current paper, employing the FSS behavior of the peaks of the sample-to-sample fluctuations of several quantities of physical (M and E_{J}) and technical (R) origin, was inspired by the intriguing analysis of Efrat and Schwartz [69]. These authors, studying also the $d = 3$ RFIM, showed that the behavior of the sample-to-sample fluctuations in a disordered system may be turned into a useful tool that can provide an independent measure to distinguish between the ordered and disordered phases of the system. The analysis of Figs. 2 and 3 above verifies their prediction, and the accuracy in the estimation of relevant phase diagram features, like the critical field h_{c} and the critical exponent ν, makes up a clear test in favor of the overall scheme.

Let us make at this point a small comment concerning the errors inherent in these types of approximations. The errors induced in the scheme based on the sample-to-sample fluctuations of Fig. 2 have their origin in the application of some polynomial, or peaklike, function in order to extract the relevant position of the maximum in the h axis. On the other hand, in similar definitions of pseudocritical points, such as through the use of some properly defined specific-heat-like quantity at $T = 0$ [74], one has to numerically differentiate the data of the bond energy E_{J}, and then consider a smoothing function to locate the position of the maximum. This scheme is subjected to two successive fitting approximations, thus increasing the errors in the estimation of the pseudocritical points.

The second part of our analysis concerns the controversial issue of the specific heat of the RFIM. The specific heat of the RFIM can be experimentally measured [15] and is, surely, of great theoretical importance. Yet it is well known that it is one of the most intricate thermodynamic quantities to deal with in numerical simulations, even when it comes to pure systems. For the RFIM, Monte Carlo methods at $T > 0$ have been used to estimate the value of its critical exponent α but were restricted to rather small systems sizes and have also revealed many serious problems, i.e., severe violations of self-averaging [62,65]. A better picture emerged throughout the years from $T = 0$ computations, proposing estimates of $\alpha \approx 0$. However, even by using the same numerical techniques, but different

scaling approaches, some inconsistencies have been recorded in the literature. The most prominent was that of Ref. [74], where a strongly negative value of the critical exponent α was estimated (see also Table II). On the other hand, experiments on random field and diluted antiferromagnetic systems suggest a clear logarithmic divergence of the specific heat [15].

In general, one expects that the finite-temperature definition of the specific heat C can be extended to $T = 0$, with the second derivative of $\langle E \rangle$ with respect to temperature being replaced by the second derivative of the ground-state energy density $E_{\rm gs}$ with respect to the random field h [35,74]. The first derivative $\partial E_{\rm gs}/\partial J$ is the bond energy $E_{\rm J}$, already defined above. The general FSS form assumed is that the singular part of the specific heat $C_{\rm s}$ behaves as $C_{\rm s} \sim L^{\alpha/\nu}\tilde{C}[(h - h_{\rm c})L^{1/\nu}]$. Thus, one may estimate α by studying the behavior of $E_{\rm J}$ at $h = h_{\rm c}$ [35]. The computation from the behavior of $E_{\rm J}$ is based on integrating the above scaling equation up to $h_{\rm c}$, which gives a dependence of the form

$$E_{\rm J}(L,h = h_{\rm c}) = c_1 + c_2 L^{(\alpha-1)/\nu}, \qquad (4)$$

with c_i constants. Alternatively, following the prescription of Ref. [74], one may calculate the second derivative by finite differences of $E_{\rm J}(h)$ for values of h near $h_{\rm c}$ and determine α by fitting to the maximum of the peaks in $C_{\rm s}$, which occur at $h^*_{\rm L} - h_{\rm c} \approx L^{-1/\nu}$ [similar reasoning to Eq. (3) above]. However, as already noted in Ref. [35], this latter approach may be more strongly affected by finite-size corrections, since the peaks in $C_{\rm s}$ found by numerical differentiation are somewhat above $h_{\rm c}$, and furthermore it is computationally more demanding, since one must have the values of $E_{\rm J}$ in a wide and very dense range of h values.

In the present case, where the critical value $h_{\rm c}$ is known with good accuracy from Fig. 3, the first approach seems to be more suitable to follow. In this framework we performed new simulations at the estimated critical-field value $h_{\rm c} = 2.2725$, but also in the area within the range $h_{\rm c} = 2.27$–2.275, as indicated by the error bar of our original estimate (2.2725 ± 0.0025) using seven candidate $h_{\rm c}$ values (see also first column of Table I). Numerically, we followed the recipe of Sec. II, using lattice sizes in the range $L = 24$–156 and averaging again over 50×10^3 random-field realizations for all candidate values. The numerical data for the bond energy and the relevant FSS analysis are presented in Fig. 4. The solid lines are acceptable power-law fittings of the form (4) with χ^2/d.o.f. varying in the range 0.6–1.1 and the estimates for the exponent ratio $(\alpha - 1)/\nu$ are given in the second column of Table I.

TABLE I. Critical exponent α of the $d = 3$ Gaussian RFIM at the seven candidate critical-field values $h_{\rm c}$ obtained from the FSS of the bond energy [Eq. (4) and Fig. 4] and the estimate $\nu = 1.379(24)$.

$h_{\rm c}$ candidates	$(\alpha - 1)/\nu$	α
2.27	−0.955(66)	−0.32(9)
2.271	−0.822(57)	−0.13(8)
2.272	−0.825(55)	−0.14(8)
2.2725	−0.788(52)	−0.08(7)
2.273	−0.800(78)	−0.1(1)
2.274	−0.784(50)	−0.08(7)
2.275	−0.744(57)	−0.03(7)

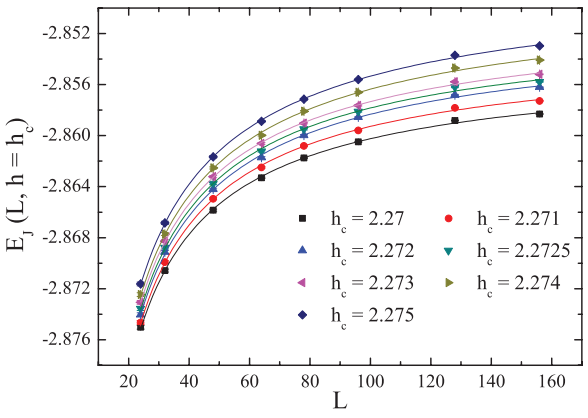

FIG. 4. (Color online) FSS behavior of the bond part of the energy density at the seven candidate values of the critical random-field strength $h_{\rm c}$. The lines are fittings of the form (4).

As in the case of Fig. 3 we also attempted here to include in our fitting attempts scaling corrections of the same form $\sim L^{-\omega}$. However, as observed in the FSS analysis of the pseudo-critical points $h^*_{\rm L}$, the fitting procedure destabilizes with the use of scaling corrections, and the fit turns out to be unacceptable. In principle, one would expect to see at least some fingerprints of the scaling corrections of the system, given the fact that the disorder-averaging process performed and the system sizes studied are considerably large. However, it turns out that is not true and that our data cannot account for the identification of scaling corrections. Since several large-scale numerical calculations [35,66,74,79], including ours, using modern algorithms on large simulation platforms have failed to deal with this issue, it seems unlikely that a numerical breakthrough will appear in the near future. Therefore, a better theoretical understanding of the system is called for, especially of corrections to scaling that may be the Achilles heel in the study of the random-field problem.

Using our estimate $\nu = 1.379(24)$, we calculate now the critical exponent α of the specific heat as a function of the candidate field $h_{\rm c}$ in the third column of Table I, obtaining estimates that lie in the interval $[-0.32(9), -0.03(7)]$, where the error bars given are of pure statistical origin (see also Table II for a summary and comparison of estimates for $h_{\rm c}$, ν, and α of the $d = 3$ Gaussian RFIM). It is clear from the values of Table I that small changes in the value of the candidate critical field can produce different values of the

TABLE II. Summary of estimates for the critical field $h_{\rm c}$, correlation length exponent ν, and critical exponent α of the specific heat obtained in the current, but also in some of the most comprehensive $T = 0$ studies, of the $d = 3$ Gaussian RFIM.

Ref.	$h_{\rm c}$	ν	α
[35]	2.270(4)	1.37(9)	−0.01(9)[a]
[66]	2.282(2)	1.25(2)	−0.05(2)
[74]	2.28(1)	1.32(7)	−0.63(7)
[79]	2.29(2)	1.1(1)	0.1(1)
This work	2.2725(25)	1.379(24)	[−0.32(9), −0.03(7)]

[a]Using the scaling of the bond energy at the mean critical field value $h_{\rm c} = 2.27$, a value of $\alpha = -0.12(16)$ has been estimated.

critical exponent α, as has also been noted in Ref. [35]. In our approach, a change in the value of h_c by a factor of $\delta h_c = 0.001$ results, on a average, in a change $\delta\alpha \approx 0.04$ in the value of α. A similar testing has been performed in Ref. [35], but with a less fine mesh. These authors showed that a change of $\delta h_c = 0.01$ introduces an uncertainty of the order of $\delta\alpha \approx 0.3$, which is compatible with our analysis and results. Thus, if one wishes to propose an estimate for the critical exponent α, corresponding to the mean value of the candidate critical field $h_c = 2.2725$, the propagation of the errors stemming from the estimation of h_c and the pure statistical errors should be taken into account, resulting in an estimate $\alpha = -0.08(24)$.

Another interesting point of Table I is that, excluding the value of α that corresponds to the case $h_c = 2.27$, all other mean α estimates are close to zero and could therefore be considered as compatible to the experimental scenario of a logarithmic divergence [15]. However, we believe that the current numerical observations do not fully account for this assessment. As already discussed, perhaps on a first approximation the identification and role of scaling corrections should be cleared out, and in a second step, new methodologies should be employed to tackle the problem. A promising route to this direction would be the application of the quotients method [92] on universal quantities, like the correlation length in units of lattice spacing. Another possibility would be the need to simulate even larger systems in order to probe safely the asymptotic regime via the route of FSS theory. Unfortunately, to the best of our knowledge, this is a task that goes far beyond the power of currently accessible computer resources.

Finally, using the modified hyper-scaling relation [19]

$$\theta = d - 1/\nu + (\alpha - 1)/\nu \tag{5}$$

and the above estimates of $(\alpha - 1)/\nu$ and the value $\nu = 1.379(24)$, we suggest the following bounds for the exponent $\theta = [1.320(47) - 1.531(41)]$, where the large range in the values stems from the propagation of the errors in the estimation of the critical field h_c. Let us note here that, if we accept the mean value $h_c = 2.2725$ for the critical field, we end up with an estimate $\theta = 1.49(3)(12)$, where the first error is purely statistical, while the second includes also the uncertainty in the estimation of h_c. This latter value of θ is compatible to the most accurate estimates in the modern literature, i.e., the values 1.49(3) of Ref. [35] for the Gaussian RFIM and 1.469(20) of Ref. [37] for the experimental analog of the RFIM, that is, the diluted antiferomagnet in a field.

In the last part of our FSS analysis, we provide a further verification of the above h_c and ν estimates, together with an independent calculation of the magnetic exponent ratios β/ν and $\bar{\gamma}/\nu$. Figure 5 illustrates a collapse behavior of the magnetization (upper panel) and disconnected susceptibility (lower panel) data, via the well-known scaling relations [73]

$$M = L^{-\beta/\nu}\tilde{M}[(h - h_c)L^{1/\nu}] \tag{6a}$$

and

$$\chi_{\rm dis} = L^{\bar{\gamma}/\nu}\tilde{\chi}_{\rm dis}[(h - h_c)L^{1/\nu}], \tag{6b}$$

where $\tilde{M}$ and $\tilde{\chi}_{\rm dis}$ are universal functions of the scaling variable $(h - h_c)L^{1/\nu}$ [91,93]. For the fitting procedure we have used *autoScale*, a program that performs a FSS analysis for given sets of simulated data [93]. The program implements a general

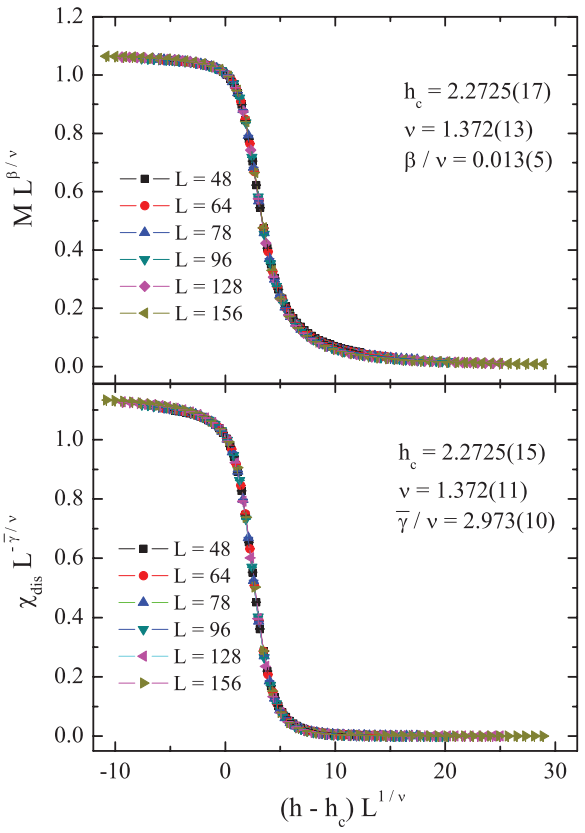

FIG. 5. (Color online) Collapse of the disorder-averaged magnetization (upper panel) and disconnected susceptibility (lower panel) data.

scaling assumption which is expected to hold best close to the critical point and optimizes an initial set of scaling parameters that enforce a data collapse of the different sets. The optimum data collapse, achieved by the minimization procedure of the scaling parameters via the downhill simplex algorithm [94], is carried out by finding a fair compromise between a (rather small) value of a χ^2/d.o.f.-like quantity, defined as S, and a reasonably large interval Δh on the rescaled abscissa. In the current case, the optimum data collapse is shown in Fig. 5 for lattice sizes in the range $L = 48$–156. The resulting values for the critical disorder strength and the correlation length exponent given in both panels of this figure are in excellent agreement with the previous estimates of Fig. 3, obtained via the FSS of the proposed pseudocritical disorder strengths h^*_L. Moreover, the values of the magnetic exponent ratios $\beta/\nu = 0.013(5)$ and $\bar{\gamma}/\nu = 2.973(10)$ compare nicely to the most accurate estimates of the literature. In particular we may refer to the best known estimates $\beta/\nu = 0.011(3)$ of Ref. [35] and $\bar{\gamma}/\nu = 2.941(46)$ of Ref. [73], both obtained by optimization methods at $T = 0$. Closing, we would like to point out that it might be also interesting to perform a data collapse analysis of the fluctuations shown in Fig. 2 using the above scaling procedure, in order to extract further estimates for the critical parameters of the system. In this case, prior to the application of the FSS program, a theoretical analysis involving the role of fluctuations in the scaling equations should provide the necessary formulae that will appear in the rescaled vertical axis.

IV. CONCLUSIONS

We have investigated the ground-state criticality of the $d = 3$ RFIM with a Gaussian distribution of fields. A scaling approach based on the sample-to-sample fluctuations of several quantities of the system allowed us to present refined estimates of the critical disorder strength h_c and the correlation length exponent ν. Particularly targeted simulations in the neighborhood of the zero-temperature critical point suggested bounds for the values of the critical exponent α of the specific heat and the violation of the hyperscaling exponent θ. Finally, accurate estimates for the magnetic exponent ratios β/ν and $\bar{\gamma}/\nu$ have been given, in good agreement with the current literature. The numerical effort recorded in the present work became feasible via the mapping of the RFIM to a network and its solution through a modified version of the push-relabel algorithm. This scheme enabled us to simulate, for a wide range of the random-field strength h, large systems, containing up to 156^3 spins, and to average over huge ensembles of realizations, increasing the statistics of ground states by a factor of 10^3, compared to previous studies of the model. Although the present computational task pushes available computing resources and goes beyond the limit of typical Monte Carlo schemes, there are still many boundaries to overcome in order to reach a complete resolution of the model's critical behavior, the most important of which is the identification and impact of scaling corrections. We are currently working towards this direction on a twofold, numerical and theoretical, basis.

ACKNOWLEDGMENTS

I.G. acknowledges financial support by Marie Curie ITN-COMPLOIDS (Grant Agreement No. 234810). N.G.F. thanks Prof. W. Selke for useful comments on the paper.

[1] Y. Imry and S.-K. Ma, Phys. Rev. Lett. **35**, 1399 (1975).
[2] A. Aharony, Y. Imry, and S.-K. Ma, Phys. Rev. Lett. **37**, 1364 (1976).
[3] A. P. Young, J. Phys. C: Solid State Phys. **10**, L257 (1977).
[4] S. Fishman and A. Aharony, J. Phys. C: Solid State Phys. **12**, L729 (1979).
[5] G. Parisi and N. Sourlas, Phys. Rev. Lett. **43**, 744 (1979).
[6] J. L. Cardy, Phys. Rev. B **29**, 505 (1984).
[7] J. Z. Imbrie, Phys. Rev. Lett. **53**, 1747 (1984).
[8] M. Schwartz and A. Soffer, Phys. Rev. Lett. **55**, 2499 (1985); Phys. Rev. B **33**, 2059 (1986); M. Schwartz, J. Phys. C: Solid State Phys. **18**, 135 (1985); M. Schwartz, M. Gofman, and T. Nattermann, Physica A **178**, 6 (1991); M. Schwartz, Europhys. Lett. **15**, 777 (1994).
[9] M. Gofman, J. Adler, A. Aharony, A. B. Harris, and M. Schwartz, Phys. Rev. Lett. **71**, 1569 (1993).
[10] J. Esser, U. Nowak, and K. D. Usadel, Phys. Rev. B **55**, 5866 (1997).
[11] W. C. Barber and D. P. Belanger, J. Magn. Magn. Mater. **226**, 545 (2001).
[12] D. P. Belanger and A. P. Young, J. Magn. Magn. Mater. **100**, 272 (1991).
[13] H. Rieger, in *Annual Reviews of Computational Physics II*, edited by D. Stauffer (World Scientific, Singapore, 1995), p. 295.
[14] See, e.g., the articles by D. P. Belanger and T. Nattermann, in *Spin Glasses and Random Fields*, edited by A. P. Young (World Scientific, Singapore, 1998), p. 251.
[15] D. P. Belanger, A. R. King, V. Jaccarino, and J. L. Cardy, Phys. Rev. B **28**, 2522 (1983); D. P. Belanger and Z. Slanič, J. Magn. Magn. Mater. **186**, 65 (1998).
[16] R. L. C. Vink, K. Binder, and H. Löwen, Phys. Rev. Lett. **97**, 230603 (2006).
[17] J. Villain, Phys. Rev. Lett. **52**, 1543 (1984); J. Physique **46**, 1843 (1985).
[18] A. J. Bray and M. A. Moore, J. Phys. C: Solid State Phys. **18**, L927 (1985).
[19] D. S. Fisher, Phys. Rev. Lett. **56**, 416 (1986).
[20] A. N. Berker and S. R. McKay, Phys. Rev. B **33**, 4712 (1986).
[21] J. Bricmont and A. Kupiainen, Phys. Rev. Lett. **59**, 1829 (1987).
[22] M. E. J. Newman, B. W. Roberts, G. T. Barkema, and J. P. Sethna, Phys. Rev. B **48**, 16533 (1993).
[23] J. Machta, M. E. J. Newman, and L. B. Chayes, Phys. Rev. E **62**, 8782 (2000).
[24] M. E. J. Newman and G. T. Barkema, Phys. Rev. E **53**, 393 (1996).
[25] M. Itakura, Phys. Rev. B **64**, 012415 (2001).
[26] N. G. Fytas and A. Malakis, Eur. Phys. J. B **61**, 111 (2008).
[27] A. Aharony, Phys. Rev. B **18**, 3318 (1978); **18**, 3328 (1978); T. Schneider and E. Pytte, *ibid*. **15**, 1519 (1977); D. Andelman, *ibid*. **27**, 3079 (1983).
[28] S. Galam and J. L. Birman, Phys. Rev. B **28**, 5322 (1983).
[29] V. K. Saxena, Phys. Rev. B **30**, 4034 (1984).
[30] A. Houghton, A. Khurana, and F. J. Seco, Phys. Rev. Lett. **55**, 856 (1985).
[31] D. C. Mattis, Phys. Rev. Lett. **55**, 3009 (1985).
[32] M. Kaufman, P. E. Klunzinger, and A. Khurana, Phys. Rev. B **34**, 4766 (1986).
[33] R. M. Sebastianes and V. K. Saxena, Phys. Rev. B **35**, 2058 (1987).
[34] A. S. de Arruda, W. Figueiredo, R. M. Sebastianes, and V. K. Saxena, Phys. Rev. B **39**, 4409 (1989).
[35] A. A. Middleton and D. S. Fisher, Phys. Rev. B **65**, 134411 (2002).
[36] R. L. C. Vink, T. Fischer, and K. Binder, Phys. Rev. E **82**, 051134 (2010).
[37] L. A. Fernández, V. Martín-Mayor, and D. Yllanes, Phys. Rev. B **84**, 100408(R) (2011).
[38] N. G. Fytas, A. Malakis, and K. Eftaxias, J. Stat. Mech.: Theory Exp. (2008) P03015.
[39] H. Rieger and A. P. Young, J. Phys. A: Math. Gen. **26**, 5279 (1993); H. Rieger, Phys. Rev. B **52**, 6659 (1995).
[40] A. Falicov, A. N. Berker, and S. R. McKay, Phys. Rev. B **51**, 8266 (1995).
[41] M. R. Swift, A. J. Bray, A. Martian, M. Cieplak, and J. R. Banavar, Europhys. Lett. **38**, 273 (1997).

[42] J.-C. Anglés d Auriac and N. Sourlas, Europhys. Lett. **39**, 473 (1997); N. Sourlas, Comput. Phys. Commun. **121**, 183 (1999).
[43] U. Nowak and K. D. Usadel, J. Esser, Physica A **250**, 1 (1998).
[44] P. M. Duxbury and J. H. Meinke, Phys. Rev. E **64**, 036112 (2001).
[45] L. Hernández and H. Ceva, Physica A **387**, 2793 (2008).
[46] N. Crokidakis and F. D. Nobre, J. Phys.: Condens. Matter **20**, 145211 (2008); O. R. Salmon, N. Crokidakis, and F. D. Nobre, *ibid.* **21**, 056005 (2009).
[47] I. A. Hadjiagapiou, Physica A **390**, 2229 (2011); **390**, 3204 (2011); **391**, 3541 (2012).
[48] Ü. Akinci, Y. Yüksel, and H. Polat, Phys. Rev. E **83**, 061103 (2011).
[49] M. Tissier and G. Tarjus, Phys. Rev. Lett. **107**, 041601 (2011).
[50] A. K. Hartmann and K. D. Usadel, Physica A **214**, 141 (1995); A. K. Hartmann, *ibid.* **248**, 1 (1998).
[51] S. Bastea and P. M. Duxbury, Phys. Rev. E **58**, 4261 (1998); S. Bastea, *ibid.* **58**, 7978 (1998); S. Bastea and P. M. Duxbury, *ibid.* **60**, 4941 (1999).
[52] R. Brout, Phys. Rev. **115**, 824 (1959).
[53] K. Binder and A. P. Young, Rev. Mod. Phys. **58**, 837 (1986).
[54] I. Dayan, M. Schwartz, and A. P. Young, J. Phys. A: Math. Gen. **26**, 3093 (1993).
[55] S. Wiseman and E. Domany, Phys. Rev. E **52**, 3469 (1995).
[56] A. Aharony and A. B. Harris, Phys. Rev. Lett. **77**, 3700 (1996).
[57] K. Eichhorn and K. Binder, J. Phys.: Condens. Matter **8**, 5209 (1996).
[58] F. Pázmándi, R. T. Scalettar, and G. T. Zimányi, Phys. Rev. Lett. **79**, 5130 (1997).
[59] S. Wiseman and E. Domany, Phys. Rev. Lett. **81**, 22 (1998).
[60] H. G. Ballesteros, L. A. Fernández, V. Martín-Mayor, A. Muñoz Sudupe, G. Parisi, and J. J. Ruiz-Lorenzo, Phys. Rev. B **58**, 2740 (1998).
[61] Y. Tomita and Y. Okabe, Phys. Rev. E **64**, 036114 (2001).
[62] G. Parisi and N. Sourlas, Phys. Rev. Lett. **89**, 257204 (2002); G. Parisi, M. Picco, and N. Sourlas, Europhys. Lett. **66**, 465 (2004).
[63] P. E. Berche, C. Chatelain, B. Berche, and W. Janke, Eur. Phys. J. B **38**, 463 (2004).
[64] C. Monthus and T. Garel, Eur. Phys. J. B **48**, 393 (2005).
[65] A. Malakis and N. G. Fytas, Phys. Rev. E **73**, 016109 (2006).
[66] Y. Wu and J. Machta, Phys. Rev. Lett. **95**, 137208 (2005); Phys. Rev. B **74**, 064418 (2006).
[67] A. Gordillo-Guerrero and J. J. Ruiz-Lorenzo, J. Stat. Mech.: Theory Exp. (2007) P06014.
[68] N. G. Fytas and A. Malakis, Phys. Rev. E **81**, 041109 (2010); Eur. Phys. J. B **79**, 13 (2011).
[69] A. Efrat and M. Schwartz, arXiv:cond-mat/0608435.
[70] A. K. Hartmann and H. Rieger, *Optimization Algorithms in Physics* (Wiley-VCH, Berlin, 2004).
[71] A. K. Hartmann and M. Weigt, *Phase Transitions in Combinatorial Optimization Problems* (Wiley-VCH, Berlin, 2005).
[72] A. T. Ogielski, Phys. Rev. Lett. **57**, 1251 (1986).
[73] A. K. Hartmann and U. Nowak, Eur. Phys. J. B **7**, 105 (1999).
[74] A. K. Hartmann and A. P. Young, Phys. Rev. B **64**, 180404 (2001).
[75] A. K. Hartmann, Phys. Rev. B **65**, 174427 (2002).
[76] E. T. Seppälä and M. J. Alava, Phys. Rev. E **63**, 066109 (2001); E. T. Seppälä, M. J. Alava, and P. M. Duxbury, *ibid.* **63**, 066110 (2001); E. T. Seppälä, A. M. Pulkkinen, and M. J. Alava, Phys. Rev. B **66**, 144403 (2002).
[77] A. A. Middleton, Phys. Rev. Lett. **88**, 017202 (2001).
[78] A. A. Middleton, arXiv:cond-mat/0208182; J. H. Meinke and A. A. Middleton, arXiv:cond-mat/0502471; D. C. Hambrick, J. H. Meinke, and A. A. Middleton, arXiv:cond-mat/0501269.
[79] I. Dukovski and J. Machta, Phys. Rev. B **67**, 014413 (2003).
[80] M. J. Alava, P. M. Duxbury, C. F. Moukarzel, and H. Rieger, in *Phase Transitions and Critical Phenomena*, Vol. 18, edited by C. Domb and J. L. Lebowitz (Academic Press, San Diego, 2001), p. 143.
[81] M. Zumsande, M. J. Alava, and A. K. Hartmann, J. Stat. Mech.: Theory Exp. (2008) P02012.
[82] G. P. Shrivastav, S. Krishnamoorthy, V. Banerjee, and S. Puri, Europhys. Lett. **96**, 36003 (2011).
[83] B. Ahrens and A. K. Hartmann, Phys. Rev. B **83**, 014205 (2011); **84**, 144202 (2011); **85**, 224421 (2012).
[84] J. D. Stevenson and M. Weigel, Europhys. Lett. **95**, 40001 (2011); Comput. Phys. Commun. **182**, 1879 (2011).
[85] N. G. Fytas, P. E. Theodorakis, and I. Georgiou, Eur. Phys. J. B **85**, 349 (2012).
[86] J.-C. Anglés d Auriac, M. Preissmann, and R. Rammal, J. Phys. Lett. **46**, L173 (1985).
[87] T. H. Cormen, C. E. Leiserson, and R. L. Rivest, *Introduction to Algorithms* (MIT Press, Cambridge, MA, 1990).
[88] C. H. Papadimitriou, *Computational Complexity* (Addison-Wesley, Reading, MA, 1994).
[89] A. V. Goldberg and R. E. Tarjan, J. Assoc. Comput. Mach. **35**, 921 (1988); B. V. Cherkassky and A. V. Goldberg, Algorithmica **19**, 390 (1997).
[90] O. Perković, K. A. Dahmen, and J. P. Sethna, Phys. Rev. B **59**, 6106 (1999); F. J. Pérez-Reche and E. Vives, *ibid.* **67**, 134421 (2003).
[91] M. N. Barber, in *Phase Transitions and Critical Phenomena*, edited by C. Domb and J. L. Lebowitz, Vol. 8 (Academic, New York, 1983), p. 146.
[92] H. B. Ballesteros *et al.*, Phys. Lett. B **378**, 207 (1996); Nucl. Phys. B **483**, 707 (1997).
[93] O. Melchert, arXiv:0910.5403.
[94] J. A. Nelder and R. Mead, Comput. J. **7**, 308 (1965).